

Back to the roots of nonclassicality

T. Kiesel, W. Vogel

Arbeitsgruppe Quantenoptik, Institut für Physik, Universität Rostock, D-18051 Rostock, Germany

V. Parigi^{1,2}, A. Zavatta^{2,3}, M. Bellini^{2,3}

¹ Department of Physics, University of Florence, I-50019 Sesto Fiorentino, Florence, Italy

² LENS, Via Nello Carrara 1, 50019 Sesto Fiorentino, Florence, Italy and

³ Istituto Nazionale di Ottica Applicata - CNR, L.go E. Fermi, 6, I-50125, Florence, Italy

A quantum state is nonclassical if its Glauber-Sudarshan P -function fails to be interpreted as a probability density. This quantity is often highly singular, so that its reconstruction is a demanding task. Here we present the first experimental determination of a well-behaved P -function showing negativities for a single-photon-added thermal state. This is a direct visualization of the original definition of nonclassicality.

PACS numbers: 03.65.Wj, 42.50.Dv, 03.65.Ta, 42.50.Xa

Einstein's hypothetical introduction of light quanta, the photons, was the first step towards the consideration of nonclassical properties of radiation [1]. But what does nonclassicality mean in a general sense? A radiation field is called nonclassical when its properties cannot be understood within the framework of the classical stochastic theory of electromagnetism. For other systems nonclassicality can be defined accordingly. Here we will focus our attention on harmonic quantum systems, such as radiation fields or quantum mechanical oscillators, for example trapped atoms.

In this context the coherent states, first considered by Schrödinger in the form of wave packets [2], play an important role. They represent those quantum states that are most closely related to the classical behavior of an oscillator or an electromagnetic wave. For a single radiation mode, the coherent states $|\alpha\rangle$ are defined as the right-hand eigenstates of the non-Hermitian photon annihilation operator \hat{a} , $\hat{a}|\alpha\rangle = \alpha|\alpha\rangle$, cf. e.g. [3]. A general mixed quantum state $\hat{\rho}$,

$$\hat{\rho} = \int d^2\alpha P(\alpha) |\alpha\rangle\langle\alpha|, \quad (1)$$

can be characterized by the Glauber-Sudarshan P -function [3, 4]. In this form the quantum statistical averages of normally-ordered operator functions can be written as

$$\langle : \hat{f}(\hat{a}, \hat{a}^\dagger) : \rangle = \int d^2\alpha P(\alpha) f(\alpha, \alpha^*), \quad (2)$$

where the normal ordering prescription, $: \hat{f}(\hat{a}, \hat{a}^\dagger) :$, means that all creation operators \hat{a}^\dagger are to be ordered to the left of all annihilation operators \hat{a} .

Formally the resulting expressions (2) for expectation values are equivalent to classical statistical mean values. However, in general, the P -function does not exhibit all the properties of a classical probability density. It can become negative or even highly singular. Within the chosen representation of the theory, the failure of the Glauber-Sudarshan P -function to show the properties of a probability density is taken as the key signature of quantumness [5, 6].

In this letter we demonstrate the first experimental determination of a nonclassical P -function. Within the experimen-

tal precision it clearly attains negative values. This is a direct demonstration of nonclassicality: the negativity of the P -function prevents its interpretation as a classical probability density.

Why is it so difficult to demonstrate the nonclassicality directly on the basis of this original definition? Let us go back to the quantum state of the photon postulated by Einstein. Its P -function is of the form

$$P(\alpha) = \left(1 + \frac{\partial}{\partial\alpha} \frac{\partial}{\partial\alpha^*}\right) \delta(\alpha), \quad (3)$$

cf. e.g. [7]. Already for a single photon we get a highly singular distribution in terms of derivatives of the δ -distribution, which cannot be interpreted as a classical probability. Due to these properties, it is difficult to experimentally determine nonclassical P -functions in general.

How can one realize nonclassical states whose properties can be demonstrated directly in terms of the original definition, that the P -function fails to be a probability density? Let a nonclassical state with a highly singular P -function propagate through a properly chosen medium. If the interaction with the medium leads to thermalization, the P -function often becomes regular, but still shows signatures of nonclassicality. Alternatively, one may start with a thermal state $\hat{\rho}_{\text{th}}$ with mean photon number \bar{n} . By photon creation one gets a single-photon-added thermal state (SPATS), $\hat{\rho} = \mathcal{N} \hat{a}^\dagger \hat{\rho}_{\text{th}} \hat{a}$, where \mathcal{N} denotes the normalization. Its P -function is well-behaved, but violates the properties of a classical probability density [8],

$$P(\alpha) = \frac{1}{\pi \bar{n}^3} [(1 + \bar{n})|\alpha|^2 - \bar{n}] e^{-|\alpha|^2/\bar{n}}, \quad (4)$$

giving rise to the question whether its experimental determination could be possible [9]. In the zero-temperature limit, the SPATS includes the special case of the one-photon Fock state with the highly singular P -function given in Eq. (3). In this sense the SPATS represents a single photon whose P -function is regularized by a controlled thermal background.

Recently SPATSs could be realized experimentally and some of their nonclassical signatures have been verified [10].

Nevertheless, the reconstruction of a nonclassical P -function remains a challenging problem which goes beyond the standard procedures of quantum state reconstruction, for the latter cf. e.g. [7]. A successful determination of the P -function of SPATS would visualize the basic definition of nonclassicality for a quantum state that lies at the heart of Einstein's hypotheses: a regularized version of a single photon.

The core of the experimental apparatus used to produce SPATSs is an optical parametric amplifier based on a type-I BBO crystal pumped by a spatially and frequency filtered laser beam at 393 nm (see Fig.1). The pump is obtained by second harmonic generation in a LBO crystal of a mode-locked Ti:Sa laser emitting 1.5 ps pulses with a repetition rate of 82 MHz. When the parametric amplifier is not injected, spontaneous parametric down-conversion takes place, generating pairs of photons at the same wavelength of the laser source along two directions commonly called signal and idler channels. We perform a conditional preparation of the quantum states by placing an on/off photodetector (D) after narrow spectral/spatial filters (F) along the idler channel [10, 11]. A

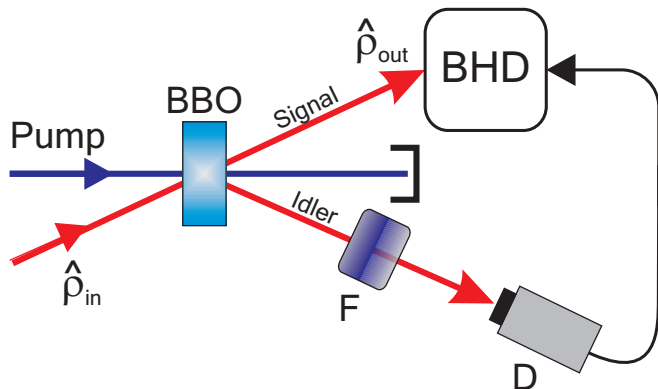


Figure 1: Scheme for the conditional excitation of a thermal light state (denoted by $\hat{\rho}_{in}$) by a single photon. A click in the on/off detector D prepares the photon-added thermal state $\hat{\rho}_{out}$ and triggers its balanced homodyne detection (BHD).

click of the idler detector prepares the signal state, which is then measured using a balanced homodyne detection scheme. The signal is mixed with a strong, mode-matched, coherent state (local oscillator, LO) by means of a 50% beam-splitter (BS). The BS outputs are detected by two proportional photodiodes connected to a home-made amplifier which provides the difference signal between the two photocurrents on a pulse-to-pulse basis [12]. The corresponding electrical signals, proportional to the quadrature operator values of the analyzed state, are then acquired and stored on a digital scope. The state is analyzed by acquiring about 10^5 quadrature values with random LO phases. When no fields are present at the inputs of the parametric amplifier, conditioned single-photon Fock states are spontaneously generated in the signal channel [11, 13]. On the other hand, we have recently shown that the injection of pure or mixed states results in the conditional production of their single-photon-added versions, al-

ways converting the initial states into nonclassical ones. In such cases, the increase in the rate of state production due to the onset of stimulated emission can also be conveniently used to absolutely calibrate the mean photon number of the input states [10, 14, 15].

Here we use a pseudo-thermal source, obtained by inserting a rotating ground glass disk in a portion of the laser beam, for injecting the parametric amplifier and producing SPATSs. The scattered light forms a random spatial distribution of speckles whose average size is larger than the core diameter of a single-mode fiber used to collect it. When the ground glass disk rotates, light exits the fiber in a clean collimated spatial mode with random amplitude and phase fluctuations yielding the photon distribution typical of a thermal source [16]. The product between the SPATS preparation rate and the coherence time of the injected thermal state (a few microseconds, and depending on the rotation speed of the disk) is kept much smaller than one. This condition assures that each state is prepared by adding a single photon to a coherent state having an amplitude and phase which are completely uncorrelated with respect to those of the previous one. This experimental realization of a thermal state directly recalls its P -function definition, i.e. a statistical mixture of coherent states weighted by a Gaussian distribution: $P(\alpha) = \exp(-|\alpha|^2/\bar{n})/(\bar{n}\pi)$.

By performing measurements on single-photon Fock states and on unconditioned thermal ones, we have estimated an overall experimental efficiency of 0.62 ± 0.04 . Both the limited efficiency in the state preparation (≈ 0.92) and in homodyne detection (≈ 0.67) degrade the expected final state by mixing it with unwanted vacuum contributions. As shown below, this does not contaminate the obtained P -function.

Let us now proceed with the reconstruction of the P -function. As the first step we calculate the characteristic function of the measured state, defined as the Fourier transform of the P -function. It can be directly obtained from the sample of N measured quadrature values $\{x_j\}_{j=1}^N$ via

$$\bar{\Phi}(\beta) = \frac{1}{N} \sum_{j=1}^N e^{i|\beta|x_j} e^{|\beta|^2/2}. \quad (5)$$

The variance of this quantity can be estimated as

$$\sigma^2 \{\bar{\Phi}(\beta)\} = \frac{1}{N} \left[e^{|\beta|^2} - |\bar{\Phi}(\beta)|^2 \right]. \quad (6)$$

In Fig. 2 we show the resulting experimental curve, which is in good agreement with the expected characteristic function $\Phi(\beta)$ for the SPATS,

$$\Phi(\beta) = (1 - (1 + \bar{n})|\beta|^2) e^{-\bar{n}|\beta|^2}, \quad (7)$$

for the mean photon number $\bar{n} = 1.11$ and the global quantum efficiency $\eta = 0.60$. We note that $|\Phi(\beta)|$ is smaller than the characteristic function of the ground state, $|\Phi(\beta)| < \Phi_{vac}(\beta) \equiv 1$. The violation of this condition would be a clear signature of nonclassicality [17]. However, this does not mean that the state is a classical one. This criterion is just the lowest

order of an infinite hierarchy of inequalities [18], see also the related theoretical and experimental results in [19] and [10], respectively.

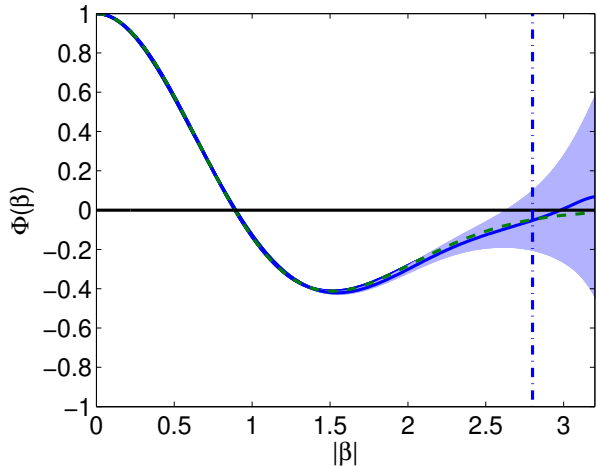


Figure 2: Experimental characteristic function (solid line) and best fit to that of a SPATS with $\bar{n} = 1.11$ and $\eta = 0.60$ (dashed line). The shaded area shows the standard deviation, the cutoff at $|\beta|_c = 2.8$ (dash-dotted line) is used for the reconstruction of the P -function.

The P -function is derived by inverse Fourier transform of

$$\sigma^2 \{ \bar{P}(\alpha) \} = \frac{1}{N} \left[\frac{4}{\pi^2} \iint_0^{|\beta|_c} bb' J_0(2b|\alpha|) J_0(2b'|\alpha|) \bar{\Phi}(b-b') e^{bb'} db db' - \bar{P}(\alpha)^2 \right]. \quad (11)$$

The reconstructed P -function is shown in Fig. 3, as derived from the experimental characteristic function given in Fig. 2. Since SPATSs do not depend on the phase, the P -representation is phase-independent as well. It is clearly seen that the P -function attains negative values, so that it fails to have the properties of a classical probability density. This is a direct proof of the nonclassicality of the experimentally realised SPATS, based on the original definition of nonclassicality [5, 6].

For a more careful discussion, we also examine a cross-section along a radial line, as shown in Fig. 4. The experimentally determined curve is drawn with the solid line. Obviously, it is in good agreement with the theoretical expectation (dashed curve). The crucial point is that we observe a distinct negative minimum at the origin of the complex α -plane. The distance between the minimum value and the $|\alpha|$ -axis is approximately equal to five standard deviations. This statistically significant negativity of the curve at the origin of the complex plane prevents the P -function from being interpreted as a classical probability density, which is a clear evidence of

$\Phi(\beta)$, which for many nonclassical states does not exist as a well-behaved function. Making use of the radial symmetry of the state, the general two-dimensional Fourier transform reduces to the Hankel-transform [20],

$$P(\alpha) = \frac{2}{\pi} \int_0^\infty b J_0(2b|\alpha|) \Phi(b) db. \quad (8)$$

In our treatment we set the experimental curve to zero for arguments greater than the cutoff value of $|\beta|_c = 2.8$, where the graph becomes negligibly small. This limits the disturbing sampling noise on the reconstructed function

$$\bar{P}(\alpha) = \frac{2}{\pi} \int_0^{|\beta|_c} b J_0(2b|\alpha|) \bar{\Phi}(b) db \quad (9)$$

to a reasonable level. The resulting systematic error

$$\Delta_P(\alpha) = \frac{2}{\pi} \int_{|\beta|_c}^\infty b J_0(2b|\alpha|) \Phi(b) db. \quad (10)$$

has been estimated with the help of the fitted theoretical function and turns out to be very small compared to the statistical fluctuations. The corresponding variance has been calculated as

nonclassicality per definition.

Let us turn to the question of how sensitively the shown negativities of the P -function depend on the precise value of the overall quantum efficiency η . The data analyzed here has been recorded by balanced homodyne detection, which is able to measure the "true" state quadratures when the efficiency is unity. For imperfect detection ($\eta < 1$), the measured statistics represents a convolution of the quadrature distribution with a Gaussian noise distribution, whose width increases with decreasing values of η , cf. [21]. Reconstructing the Wigner-function of a given quantum state, the increasing noise due to a decrease of the quantum efficiency smoothes out the structures of the Wigner-function and may hide the nonclassical effects. It is of great importance that such a problem is absent in the reconstruction of the P -function. The latter has the property that both its shape and the relative noise level do not depend on the value of the quantum efficiency, losses only lead to a rescaling of the quadrature variable, cf. e.g. [22]. The P -function obtained by perfect detection is related to $P_\eta(\alpha)$, obtained with the quantum efficiency η , via $P(\alpha) = \eta P_\eta(\sqrt{\eta}\alpha)$. Hence the nonclassical effects are preserved even for a small

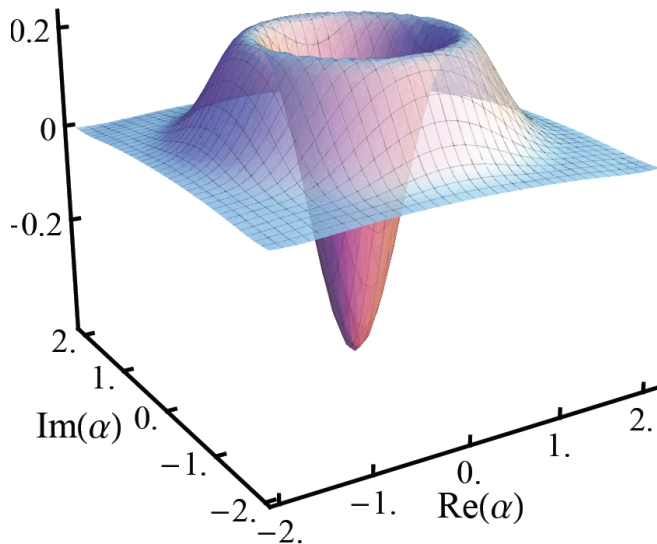


Figure 3: Experimentally reconstructed P -function of a SPATS.

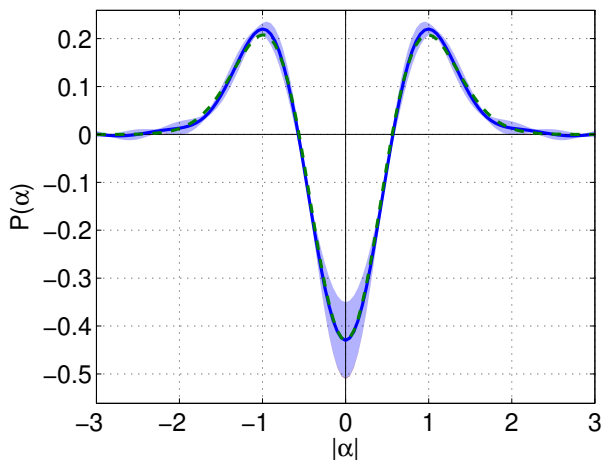


Figure 4: The experimentally reconstructed P -function of a SPATS (solid line) is compared with a theoretical fit (dashed line) for $\bar{n} = 1.11$ and $\eta = 0.60$. Both curves agree within one standard deviation (shaded area).

efficiency. For other phase-space distributions, such as the Wigner-function, this property is lost.

In conclusion, we have reconstructed the Glauber-Sudarshan P -function of an experimentally prepared single-photon-added thermal state. We obtain a well-behaved function with statistically significant negativities, so that it fails to show the properties of a classical probability density. This is the first direct demonstration of nonclassicality according to its original definition.

This work was partially supported by Ente Cassa di Risparmio di Firenze and MIUR, under the PRIN initiative.

-
- [1] A. Einstein, *Ann. Phys.* **17**, 132 (1905).
 - [2] E. Schrödinger, *Naturwiss.* **14**, 664 (1926).
 - [3] R. J. Glauber, *Phys. Rev.* **131**, 2766 (1963).
 - [4] E. C. G. Sudarshan, *Phys. Rev. Lett.* **10**, 277 (1963).
 - [5] U. M. Titulaer and R. J. Glauber, *Phys. Rev.* **140**, B676 (1965).
 - [6] L. Mandel, *Phys. Scr.* **T12**, 34 (1986).
 - [7] W. Vogel and D.-G. Welsch, *Quantum Optics* (Wiley-VCH, 2006), 3rd ed.
 - [8] G. S. Agarwal and K. Tara, *Phys. Rev. A* **46**, 485 (1992).
 - [9] T. Richter, *J. Mod. Opt.* **48**, 1881 (2001).
 - [10] A. Zavatta, V. Parigi, and M. Bellini, *Phys. Rev. A* **75**, 052106 (2007).
 - [11] A. Zavatta, S. Viciani, and M. Bellini, *Phys. Rev. A* **70**, 053821 (2004).
 - [12] A. Zavatta, M. Bellini, P. L. Ramazza, F. Marin, and F. T. Arecchi, *J. Opt. Soc. Am. B* **19**, 1189 (2002).
 - [13] A. I. Lvovsky, H. Hansen, T. Aichele, O. Benson, J. Mlynek and S. Schiller, *Phys. Rev. Lett.* **87**, 050402 (2002).
 - [14] A. Zavatta, S. Viciani, and M. Bellini, *Science* **306**, 660 (2004).
 - [15] V. Parigi, A. Zavatta, M. S. Kim, and M. Bellini, *Science* **317**, 1890 (2007).
 - [16] F. T. Arecchi, *Phys. Rev. Lett.* **15**, 912 (1965).
 - [17] W. Vogel, *Phys. Rev. Lett.* **84**, 1849 (2000).
 - [18] T. Richter and W. Vogel, *Phys. Rev. Lett.* **89**, 283601 (2002).
 - [19] E. Shchukin, T. Richter and W. Vogel, *J. Opt. B* **6**, S597 (2004).
 - [20] A. J. Jerri, *Integral and discrete transforms with applications and error analysis* (Marcel Dekker, Inc., 1992).
 - [21] W. Vogel and J. Grabow, *Phys. Rev. A* **47**, 4227 (1993).
 - [22] A. A. Semenov and D. Yu. Vasylyev and B. I. Lev, *J. Opt. B* **39**, 905 (2006).